Integrating Two Spectral Imaging Systems in an Automated Mineralogy Application

Dugal Harris, Narendra Viranna, Graeme Hill
DebTech, De Beers Group Services
PO Box 82851, Southdale, 2135, South Africa
Email: graeme.hill@debeersgroup.com

Jeremy Green
CSIR
Centre for Mining Innovation (CMI)
Novel Mining Methods Group
Johannesburg, South Africa
Email: jgreen@csir.co.za

A system for the automated analysis and sorting of mineral samples has been developed to assist in the concentration of heavy mineral samples in the diamond exploration process. These samples consist of irregularly shaped mineral grains ranging from 0.3 to 1mm in diameter, and the application requires the treatment of this material at the rate of tens of grams per hour.

Specific mineral grains of interest are identified and extracted from a mineralogically highly diverse background. Material is treated in batches, with trays of mono-layered material presented to various imaging systems. The identification of target grains is achieved by means of spectral imaging in two wavelength bands (Visible, and Long Wave Infrared). Target grains are then extracted by means of a SCARA robot, in a pick-and-place arrangement.

The successful development required the solution of various challenges in the image processing and materials handling domains. A previous paper has concentrated on the physical handling of the small, irregularly shaped grains [1]. In this paper we concentrate on the imaging challenges, specifically associated with the registration between separate spectral images to a high spatial accuracy. The pick-and-place system required that the pneumatic nozzle is directed to a target position with an accuracy of 100 micron, in terms of both the particle plane and the height above the particle bed. We describe the registration and image distortion correction methodologies employed, in order to achieve this accuracy.

I. INTRODUCTION

The process of diamond exploration includes the treatment of soil samples, in order to recover indicator mineral grains. The soil samples undergo various density separation, cleaning, and sizing processes. This leaves a clean sample of mono-mineralic grains, typically in 0.300-0.500mm and 0.500-1.00mm size fractions. A typical sample from which indicators are to be recovered, ranges from tens to hundreds of grams. Currently, these samples are sorted by trained mineral sorters.

DebTech, the R&D division of De Beers, has developed a robotic system for the automatic treatment of such samples. The instrument, referred to as AMANDA, represents an integration of off-the-shelf robotics and optics, together with in-house developed components. Fundamentally, reflectance spectroscopy in the Visible (VIS) and Long Wave Infrared (LWIR) wavelength ranges is used to identify the grains of interest. DebTech has developed proprietary algorithms for the detection of the indicator minerals, based on the measured reflectance spectra from the grains.

The application requires the acquisition of VIS and LWIR spectra from each grain in the sample. These spectra, furthermore, must be co-registered, in that the VIS and LWIR spectra corresponding to a specific grain are paired correctly. Grains that are identified as targets must then be physically extracted from the rest of the sample. Because target grains are typically very rare, and so relatively few grains need to be extracted, the application lends itself to a pick-and-place embodiment.

Material handling involves presenting batches of material, on specifically designed trays, to an indexer. The indexer transfers the trays to two spectral imaging camera stations, followed by a recovery station where target grains are extracted by a pneumatic pick-and-place system.

Due to the small size of the grains (down to 300 micron), the positioning of the pick-and-place nozzle needs to be highly accurate. A design accuracy of 100 micron was chosen. This paper discusses the spectral image registration methods employed to achieve the required spatial accuracy.

II. Overview of the AMANDA Machine

AMANDA consists of the following subsystems:

Materials handling system: This system, comprising an articulated robot (EPSON Pro Six PS3 series) and a material feeding and preparation system, prepares the material in batches of approximately 1 gram. The material is prepared on a tray, with a surface area of 5 x 5 cm^2. Figure 1 shows an image of the tray at the pick-and-place station. The material has been prepared in a monolayer, by a vibrating preparation stage, for presentation to the imaging systems.

Indexing system: An indexing system, comprising a conveyer belt transfers the trays between three stations: a) the VIS spectral image acquisition station, b) the LWIR spectra acquisition station, and c) the pick-and-place station. Crucially, the particle grains on the tray remain undisturbed when transferred from station to station.

Imaging systems: AMANDA incorporates two spectral imaging systems. A spectral image is simply a set of images of the same scene, taken in consecutive, narrow wavelength bands. The spectral imaging system at the VIS station comprises a Specim Imspector V10E spectrograph, a Dalsar 1M30 scientific grade camera, with an OLE23 (23mm focal length) fore lens. This camera acquires images using the push-broom method, which involves scanning the camera across the tray, and the image is built up from a series of narrow windows. The VIS spectral image consists of 261 wavelength bands. LWIR spectral images are acquired at the Infrared station, by means of a custom designed thermal imager, developed in collaboration with Optocon Systems (Pty) Ltd. This imager, which incorporates a Miricle 307K microbolometer array from Thermoteknix, generates 6 bands of equal width, over the 8 to 14 micron range. Both spectral imaging systems have been designed to produce a pixel resolution in the region of 100 micron, meaning that 100 by 100 square microns of the object plane corresponds to 1 pixel on the detector array.

Finally, a high resolution grey scale CCD camera images the tray at the pick-and-place station. As discussed below, this image is used to transform between spectral image and the robot coordinates of the pick-and-place (PNP) system. A typical image is shown in Figure 1.

Pick-and-Place system: This comprises a SCARA robot (EPSON E2S 45 1 S), with a vacuum nozzle tool. Details of this system, including its calibration have been discussed previously [1].

III. Image Registration

There are two general approaches to registration [2]:

1. Intensity based, where correlation metrics between the pixel values of the images to be registered are used to derive the spatial transformation.
2. Feature based, where the locations of distinctive features, such as corners, are detected and used to derive the spatial transformation.

An initial study into using the intensity based approach was performed. This approach is ill-suited to the AMANDA configuration due to the intensive computational requirements and multi-modality arising from the use of VIS and LWIR sensors. The constrained AMANDA configuration allows us to follow the feature based approach as we had the freedom to place features on the particle tray. Four distinctive circular reference markers were placed on the AMANDA particle tray (see Figure 1). These markers are visible in all 3 images (VIS, LWIR, and PNP), providing a common point of reference to derive spatial transformations between the image spaces. Circles were chosen as their shape is invariant to rotation.

Some features are also required to provide a common reference between the PNP image and robot spaces. Six additional off-tray markers, which are mechanically fixed with respect to the SCARA robot coordinate system, were placed in the PNP camera field of view (see Figure 1). The off-tray markers were chosen to be three concentric circles, with the central circle recessed (dark area of marker in Figure 1) so that their locations can be measured using a displacement laser mounted on the end effector of the SCARA robot. An automated calibration sequence has been implemented, in which the robot "feels" for the positions of the off-tray markers, using feedback from the laser displacement laser.

The locations of the off-tray markers, in PNP image and robot co-ordinate space, are used to infer the corresponding spatial transform. The transformation from VIS or LWIR image space to PNP robot space is thus a 2-step process using the PNP image as an intermediate step. The VIS/LWIR image space is transformed to PNP image space and then to PNP robot space.

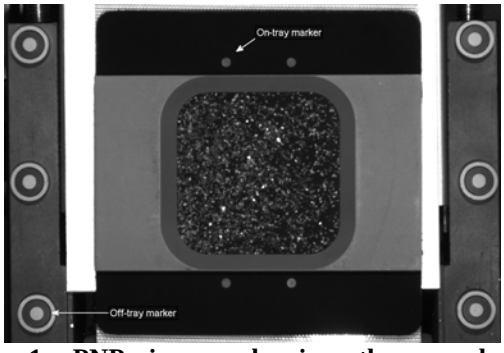

Figure 1. PNP image showing the sample tray, containing a monolayer of mineral grains. The on-tray and off-tray reference markers are indicated.

The VIS/LWIR/PNP camera pose relative to the tray can vary from tray to tray and over time. This is due to the elasticity of the belt, which results in variation in belt height and stopping position. The position at which the tray is

placed on the belt, by the articulated robot, may also vary. The projective transform [3] can describe all these variations and was therefore chosen as the form of the spatial transformation between camera/robot co-ordinate spaces. One requires a minimum of four pairs of points to determine this transformation, which is satisfied by the four on-tray markers for between camera transformations and the six off-tray markers for PNP camera to robot transformation.

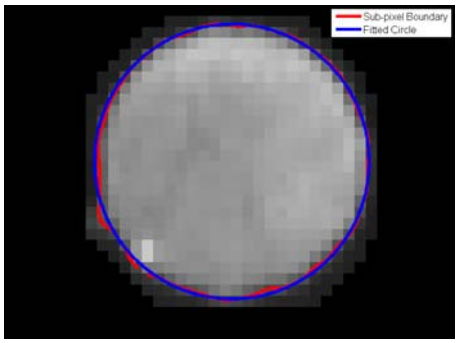

Figure 2. Sub-pixel boundary with RANSAC circle detection

Reference Marker Detection

As the VIS/LWIR to robot space registration is a 2-step procedure, the errors from each step will accumulate. The reference markers thus need to be detected to sub-pixel accuracy in each image to achieve the overall 1 pixel required accuracy. The detection algorithm also needs to be robust to non-uniformities in the marker appearance, such as dust and shadows. This section describes the algorithm used.

Due to the controlled illumination conditions, simple threshold based segmentation is sufficient to separate the markers from the tray background. A series of pre-processing steps are performed on the segmented image, to exclude the particle area of the tray and any dust lying outside this area. These steps are specific to each of the three images and are too detailed to be covered here. Sub-pixel boundaries are found in the pre-processed image using a marching square method [4]. A RANSAC algorithm [5] is then used to fit circles to the boundaries. The RANSAC circle detector was chosen as it is not biased by the presence of non-uniformities in the circle boundaries. An example of a fitted circle and sub-pixel boundary is shown in Figure 2. The centers of the markers are then found from the fitted circles. Figure 3 shows an example of these steps, including pre-processing, for the VIS image.

Distortion Correction

The AMANDA images are subject to optical distortion. The VIS image distortion is severe enough that is must be corrected in order to achieve the required overall 1 pixel accuracy. In the case of the LWIR camera, with custom designed telecentric optics, distortion is less severe. It is, however, still significant, and is therefore also corrected to help improve overall accuracy.

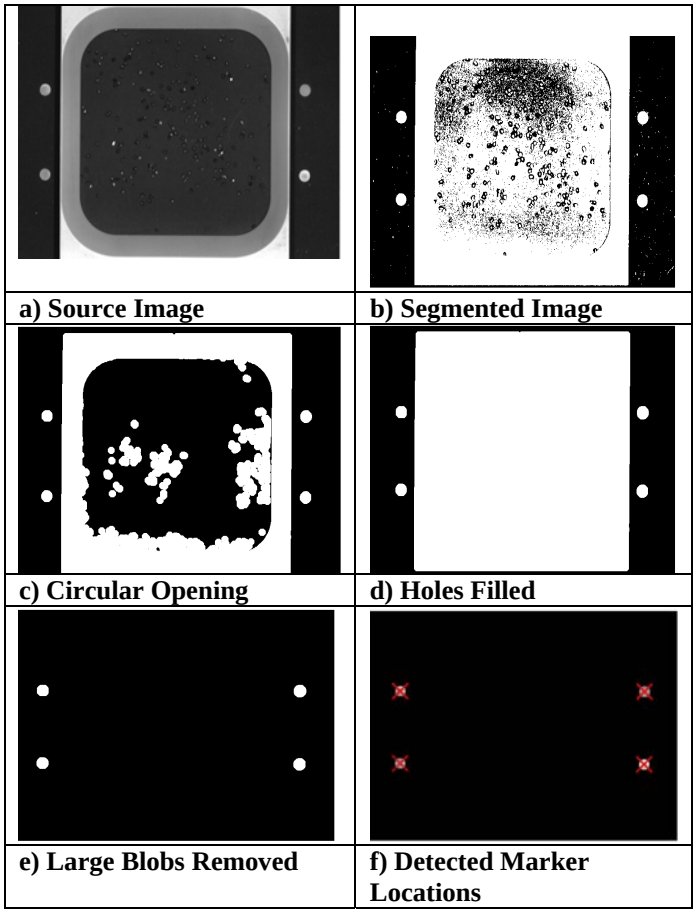

Figure 3. VIS Image Marker Detection

In contrast to the registration transformations, which must be determined for each image, the lens distortions remain consistent over time. The distortion corrections can thus be fitted once in an offline calibration step and re-used for each image. The registration transforms are then found from the undistorted images.

The observed distortion in the VIS image is not described by a conventional radial distortion model. This is because the VIS image is acquired by the push-broom method, and the distortion therefore occurs along only one dimension of the image. The lens also produces a combination of barrel and pincushion type distortions along this dimension. A polynomial model was used to represent the distortion as follows:

$$x = f_x(x', y')$$

$$y = f_y(x', y')$$

where f_x and f_y are polynomial functions, x' and y' are the observed (distorted), and x and y the target

(undistorted) image co-ordinates. This model is general enough to describe the LWIR distortion as well, which is roughly barrel type. The model is fitted to data obtained from an image of a tray inscribed with a regular grid pattern. The grid pattern covers the full field of view. The grid crossings are found using template matching with correlation. The measured co-ordinates of the grid crossings are used as the observed data and the co-ordinates of a regular grid as the target data. Polynomial terms are added to the model using a forward selection procedure with mean square error as the selection criterion [6]. To prevent overfitting, the polynomial order and number of terms are validated against independent grid images.

Figure 4 shows the target, distorted and corrected grid crossings for a portion of a VIS grid image. It can be seen that the distortion is significant and occurs mostly in the vertical dimension (The push-broom scan dimension is horizontal). The mean error distance between target and measured grid crossings before correction is 2.66(1.04) pixels and 0.17(0.10) pixels after correction for this VIS image. For an LWIR image the error before correction is typically 0.40(0.25) pixels and 0.25(0.15) after correction. (Standard deviations are given in brackets.)

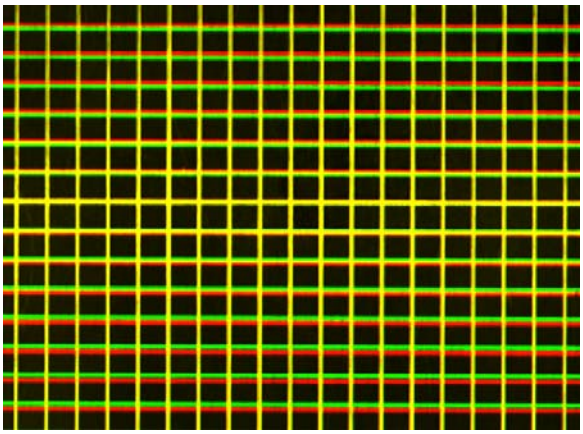

Figure 4. RGB image of distorted and corrected grid images, with the greyscale distorted image in the Red band and the greyscale corrected image in the Green band. (Yellow would therefore indicate correspondence between the corrected and uncorrected images. Green and red represent areas of significant distortion.)

IV. Results

Evaluation of combined distortion correction and registration accuracy was performed using a tray where the particle area was covered with a grid pattern. Three evaluations were performed:

1. The accuracy of the VIS image transformed to LWIR image co-ordinate space.
2. The accuracy of the VIS image transformed to PNP image co-ordinate space.
3. The accuracy of the LWIR image transformed to PNP image co-ordinate space.

The accuracies of the transformations were evaluated by calculating the median and median absolute deviation (MAD) of the pixel distance between corresponding grid crossings of the two images in the transformed space. Median measures were used to prevent spurious grid crossing detections biasing the results. The results are tabulated below and shown in Figure 5 to Figure 7.

Evaluation	Median Distance	MAD Distance
VIS – LWIR	0.48 pixels	0.22 pixels
VIS – PNP	0.34 pixels	0.16 pixels
LWIR – PNP	0.43 pixels	0.19 pixels

The achieved accuracies are within the 1 pixel limit. It is apparent that a significant contribution to transformation inaccuracy is the VIS and LWIR distortion (see distortion correction accuracy figures in section III).

The final accuracy of positioning of the nozzle will include the accuracy of the PNP image to robot space conversion. There is no significant distortion in the PNP image or robot co-ordinate spaces, and so this accuracy is determined by the accuracy of the robot calibration procedures, described in [1]. The accuracy of this calibration procedure is difficult to quantify, and so performance evaluation is based on the final accuracy of the system. An effective method employed is to drive the laser displacement meter to a target position on the tray, and observe whether the beam is directed onto the centre of the particle.

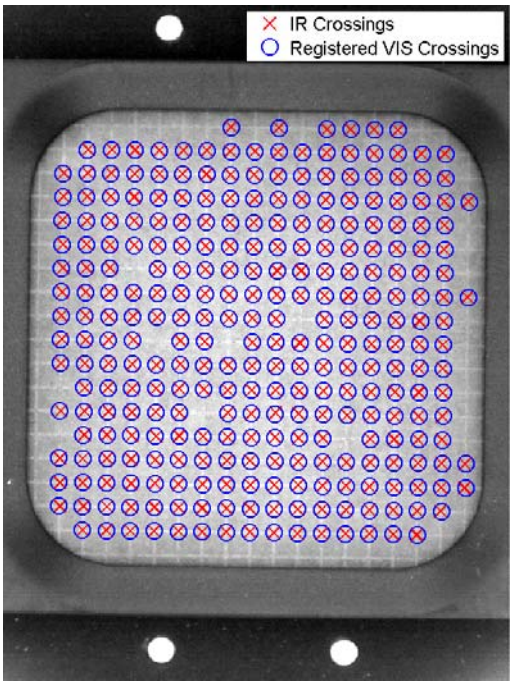

Figure 5. VIS Grid Crossings Transformed to LWIR Image Space

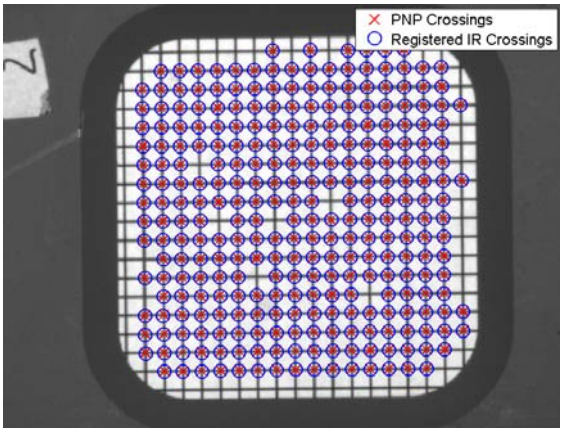

Figure 6. LWIR Grid Crossings Transformed to PNP Image Space

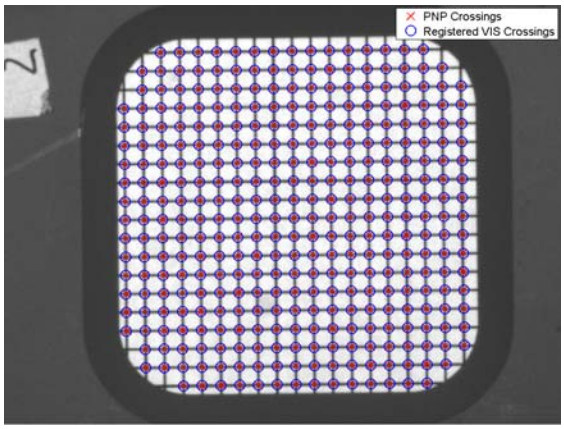

Figure 7. VIS Grid Crossings Transformed to PNP Image Space

V. CONCLUSIONS

We have demonstrated the successful registration, to sub-pixel accuracy, between two spectral imaging systems, and a third grey scale (pick-and-place station) imaging system. This allows for co-registration of the VIS and LWIR spectra of individual mineral grains. Furthermore, the registration of spectral to the pick-and-place images, together with the calibration of the SCARA robot as described in [1], allows for the placement of the vacuum nozzle to within sufficient accuracy above the target grain for successful picking.

The proof of the system is in the final sorting performance. The AMANDA system extracts grains with better than 80% success rate, and produces concentrates of a few percent by mass of the feed material. The primary cause of the missing of targets is due to spectral classification of targets, rather than the extraction system.

REFERENCES

1. Jeremy J. Green, *The Robotic Handling of Small Mineral Grains with a Vacuum Nozzle*, 2nd Robotics and Mechatronics Symposium, CSIR, November 2008
2. A. Ardeshir Goshtasby. *2-D and 3-D Image Registration for Medical, Remote Sensing, and Industrial Applications*, Wiley Press, 2005.
3. Richard Hartley and Andrew Zisserman. *Multiple View Geometry in Computer Vision*. Cambridge University Press, 2003.
4. Keith Forbes, *Calibration, Recognition, and Shape from Silhouettes of Stones.* PhD Thesis. University of Cape Town, June 2007
5. Martin A. Fischler and Robert C. Bolles. *Random Sample Consensus: A Paradigm for Model Fitting with Applications to Image Analysis and Automated Cartography*. Comm. Of the ACM 24: 381–395, June 1981.
6. S.A. Billings, S. Chen and M.J. Korenberg, *Identification of MIMO non-linear systems using a forward-regression orthogonal estimator*. Int J. of Control, 49, 2157-2189, 1988